

Control of a single-photon router via an extra cavity

Yi-Ke Luo,¹ Ya Yang,¹ Jing Lu,¹ and Lan Zhou*¹

Synergetic Innovation Center for Quantum Effects and Applications, Key Laboratory for Matter Microstructure and Function of Hunan Province, Key Laboratory of Low-Dimensional Quantum Structures and Quantum Control of Ministry of Education, School of Physics and Electronics, Institute of Interdisciplinary Studies, Hunan Normal University, Changsha 410081, China

(*Electronic mail: zhoulan@hunnu.edu.cn)

(Dated: 4 December 2023)

Controllable single-photon routing plays an important role in quantum networks. We investigate single-photon scattering in two one-dimensional (1D) waveguides by a three-level emitter with a cascade configuration, which is a dipole coupled to an extra cavity. The tunneling path for the transmission of a single photon is switched by whether the extra cavity contains photons. For the setup, the Autler-Townes splitting is modulated by the extra cavity, in which the transmission valley (reflection range) width is tunable in terms of the number of photons in the extra cavity. Our investigation will be beneficial to single-photon routing in quantum networks using quantifiable photon numbers in an extra cavity.

Quantum network, which is the essence of quantum information processing, and the key lies in the ability of quantum state transfer, that is, evaluating the effectiveness of transferring quantum states from one end to the other¹. It is well known that photons are one of the ideal candidates as information carriers for long-distance optical quantum communication due to their low decoherence rate²⁻⁴. Therefore, how to efficiently and perfectly route photon signals in quantum channels is an important topic in quantum communication. At present, the quantum router has been theoretically and experimentally studied in a variety of systems, i.e., coupled-resonator waveguides (CRWs)⁵⁻¹¹, superconducting circuits¹²⁻¹⁷, optomechanical systems¹⁸⁻²³, and atomic systems^{7,24-34}. In addition, using waveguide-QED systems^{35,36}, researchers have put forward many proposals for single-photon (SP) routing^{5,7,8,10,28,29,37-41}. The SP router with multiple channels can be achieved by controlling the driving field strength of the Λ -type three-level system (3LS) and its coupling strengths with the waveguides^{41,42}. It is interesting to study the controllable single-photon transport through the extra cavity. The Autler-Townes splitting is modulated by the extra cavity^{15,17,20,21,43-45}, and the width of the transmission valley can be adjusted by controlling the number of photons in the extra cavity.

Here, we introduce a scheme for a four-port system, which is based on quantum interference tuned by chiral waveguide-emitter coupling⁴². In this paper, the photon transport can be controlled by an extra cavity. If the extra cavity is in a vacuum state, our scheme can be regarded as two independent one-dimensional (1D) waveguides chiral coupled to a two-level system⁴⁶. However, once the extra cavity contains photons, the input single photon will appear to have more abundant transmission properties. It is shown that the full transmission of the input single photon can be obtained in the resonance case. This is the condition of the total reflection of the two-level system⁴⁶. Moreover, we analyzed the scattering spectrum of a single photon using the parameters of the extra cavity⁴⁷⁻⁵⁰, such as the coupling strength to the emitter, photon number, and resonance frequency. Incidentally, our scheme can be regarded as two 1D waveguide chiral coupled

to a V-type atom in the dressed state representation. In this way, the dressed state makes it easier to understand the physical images than the bare state. First, we present the four-port device and its Hamiltonian. Introducing the parity operator to divide it into the scatter-free subspaces and the controllable subspaces. Then we study the scattering process for a single photon and explain how to adjust the parameters of the extra cavity to realize perfect single-photon routing. Finally, we conclude with a brief summary of the results.

The system under study is depicted in Fig. 1(a): Two 1D waveguides, which we labeled a and b, respectively, chiral coupled to a cascaded three-level emitter. The cascade three-level system can be a real atom or a manual atomlike object⁵¹⁻⁵³. In the circuit quantum electrodynamics system, the three-level atom coupled to the multiple-modes can be realized by the Josephson junctions connecting to transmission lines^{6,54}. The atomic states with frequencies ω_1 , ω_2 , and ω_3 are denoted by $|1\rangle$, $|2\rangle$, and $|3\rangle$. We choose the ground-state energy $\omega_1 = 0$. In the rotating-wave approximation, the system Hamiltonian has the form ($\hbar = 1$)

$$H = H_w + H_a + H_A + H_{int}. \quad (1)$$

The first term H_w describing the free propagation of the photons is given by

$$H_w = -i \sum_{p=a,b} \int dx \left[R_p^\dagger(x) \frac{\partial}{\partial x} R_p(x) - L_p^\dagger(x) \frac{\partial}{\partial x} L_p(x) \right]. \quad (2)$$

Here we assume that the group velocities of each waveguide are equal and are set to be 1 hereafter. And $R_p^\dagger(x)$ [$L_p^\dagger(x)$] is a bosonic operator creating a right-going (left-going) photon in waveguide $p = a, b$ at x . Representing the extra cavity of resonance frequency ω_a by the annihilation operator a , its Hamiltonian is

$$H_a = \omega_a a^\dagger a. \quad (3)$$

The third term H_A gave the three-level system's Hamiltonian

$$H_A = \omega_2 \sigma_{22} + \omega_3 \sigma_{33}. \quad (4)$$

where $\sigma_{mn} = |m\rangle\langle n|$ ($m, n = 1, 2, 3$) represents the atomic energy-level population operators.

The transition from level $|2\rangle$ to $|3\rangle$ is driven by the extra cavity with driving strength λ and $\omega_{32} = \omega_3 - \omega_2$ is far from the cutoff frequency of the waveguide. It clearly shows that the waveguides and the transition $|2\rangle \leftrightarrow |3\rangle$ (the extra cavity) are decoupled from each other when $\Delta = \omega_{32} - \omega_k$ is very large. So the transition $|2\rangle \leftrightarrow |3\rangle$ doesn't exchange energy with the waveguides. Moreover, the frequency difference ω_{32} satisfies the conditions $|\omega_{32} - \omega_a| \ll |\omega_{32} + \omega_a|$. However, the frequency difference between the levels $|2\rangle$ and $|1\rangle$ is assumed below the cutoff frequency of the waveguide, hence, the guided photon is coupled to the transition $|1\rangle \leftrightarrow |2\rangle$ with coupling strength γ_{pg} ($p \in \{a, b\}, g \in \{r, l\}$). So, the interaction Hamiltonian H_{int} has the form

$$H_{int} = \sum_{p=a,b} \int dx \delta(x) [\sqrt{\gamma_{pr}} R_p^\dagger(x) + \sqrt{\gamma_{pl}} L_p^\dagger(x)] \sigma_{12} + \lambda a^\dagger \sigma_{23} + H.c. \quad (5)$$

The coupling rates to right- and left-going photons in waveguide p ($p = a, b$) are denoted by γ_{pr} and γ_{pl} , respectively (Fig. 1(a)). The couplings are chiral as long as $\gamma_{pr} \neq \gamma_{pl}$. It is widely known that if the time-reversal symmetry of the waveguide is broken by a magnetic⁵⁵⁻⁵⁷ or synthetic magnetic field⁵⁸⁻⁶⁰, then chiral couplings are achieved. When the time-reversal breaking is strong enough, the ideal chiral waveguide ($\gamma_{pg} = \gamma_p, \gamma_{p\bar{g}} = 0, \bar{g} \neq g; g, \bar{g} \in \{r, l\}$) has been demonstrated experimentally^{55-59, 61, 62}. The system we are studying belongs to the chiral QED systems, which have recently attracted widespread attention⁶³⁻⁶⁷.

We assumed that a single photon in the waveguide p is incident from the left side with momenta k , the atom is in its ground state $|1\rangle$, and the extra cavity contains n ($\lambda \sqrt{n} \ll \{\omega_{32}, \omega_a\}$) photons. Obviously, when $n = 0$, our model is equal to 1D waveguides chiral coupled to a two-level system⁶⁸. However, when $n \neq 0$, the transition $|2\rangle \leftrightarrow |3\rangle$ participates in the dynamic process, revealing different results from the $n = 0$ case.

As a first step, we introduce the parity operators

$$E^\dagger(x) = \sqrt{\frac{\gamma_{ar}}{\gamma}} R_a^\dagger(x) + \sqrt{\frac{\gamma_{al}}{\gamma}} L_a^\dagger(-x) + \sqrt{\frac{\gamma_{br}}{\gamma}} R_b^\dagger(x) + \sqrt{\frac{\gamma_{bl}}{\gamma}} L_b^\dagger(-x), \quad (6a)$$

$$O^\dagger(x) = \sqrt{\frac{\gamma_b}{\gamma_a}} \sqrt{\frac{\gamma_{ar}}{\gamma}} R_a^\dagger(x) + \sqrt{\frac{\gamma_b}{\gamma_a}} \sqrt{\frac{\gamma_{al}}{\gamma}} L_a^\dagger(-x) - \sqrt{\frac{\gamma_a}{\gamma_b}} \sqrt{\frac{\gamma_{br}}{\gamma}} R_b^\dagger(x) - \sqrt{\frac{\gamma_a}{\gamma_b}} \sqrt{\frac{\gamma_{bl}}{\gamma}} L_b^\dagger(-x), \quad (6b)$$

and

$$O_a^\dagger(x) = \sqrt{\frac{\gamma_{al}}{\gamma_a}} R_a^\dagger(x) - \sqrt{\frac{\gamma_{ar}}{\gamma_a}} L_a^\dagger(-x), \quad (7a)$$

$$O_b^\dagger(x) = \sqrt{\frac{\gamma_{bl}}{\gamma_b}} R_b^\dagger(x) - \sqrt{\frac{\gamma_{br}}{\gamma_b}} L_b^\dagger(-x), \quad (7b)$$

with $\gamma_p = \gamma_{pr} + \gamma_{pl}, \gamma = \gamma_a + \gamma_b$. By employing the above transformation, the original Hamiltonian is transformed into two decoupled Hamiltonians, i.e., $H = H_e + H_o$, where

$$H_e = H_w^e + H_a + H_A + H_{int}^e, \quad (8a)$$

$$H_w^e = -i \int dx E^\dagger(x) \frac{\partial}{\partial x} E(x), \quad (8b)$$

$$H_{int}^e = \int dx \sqrt{\gamma} \delta(x) E^\dagger(x) \sigma_{12} + \lambda a^\dagger \sigma_{23} + H.c., \quad (8c)$$

and

$$H_o = -i \int dx \left[O^\dagger(x) \frac{\partial}{\partial x} O(x) + \sum_{p=a,b} O_p^\dagger(x) \frac{\partial}{\partial x} O_p(x) \right], \quad (9)$$

with $[H_e, H_o] = 0$. So, we call H_o the interaction-free independent three-mode Hamiltonian, while H_e describes a nontrivial one-mode interacting model with coupling strength γ .

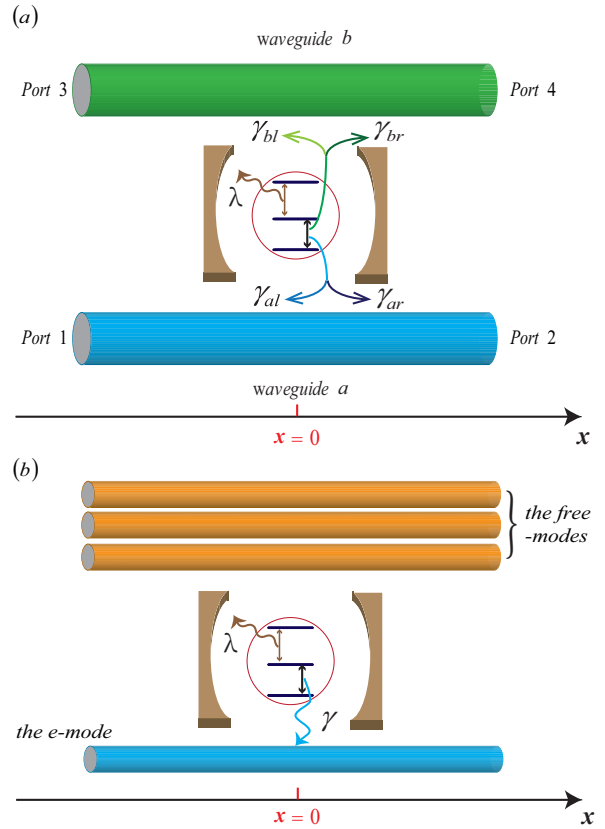


FIG. 1. (Color online) (a) Schematic of a few-photon router with four ports: A three-level system with cascade configuration interacts with two independent waveguides labeled a and b . The blue (green) line represents the chiral coupling between the level transitions $|1\rangle \leftrightarrow |2\rangle$ and the left and right-going photons of the bottom waveguide a (b), and the coupling rates are γ_{ar} (γ_{br}) and γ_{al} (γ_{bl}), respectively. (b) An equivalent few-photon router by introducing scatter-free channels and the controllable channel: The three-level system only interacts with one mode with a strength determined by γ .

The decomposition of Hamiltonian H in Eq. (1) into two parts in the previous section leads to the discussion of the

problem from one mode interacting model Hamiltonian H_e , which greatly simplifies the calculations. In this section, we will calculate the single-photon scattering process in detail. By the definition of the parity operators, types Eqs. (6-7), $R_p^\dagger(x)$ and $L_p^\dagger(x)$ can be decomposed into $E^\dagger(x)$, $O^\dagger(x)$, and $O_p^\dagger(x)$. Therefore, any one photon state $|\Psi^{(1)}\rangle$ can be written as

$$|\Psi^{(1)}\rangle = \cos\alpha |\Psi\rangle_e + \sin\alpha |\Psi\rangle_o. \quad (10)$$

One could readily write that the full interacting one-photon eigenstate $|\Psi\rangle_e$ for H_e takes the form

$$|\Psi\rangle_e = \int dx f_k(x) c_e^\dagger(x) |\otimes\rangle |1, n\rangle + \beta |\otimes\rangle |2, n\rangle + \zeta |\otimes\rangle |3, n-1\rangle, \quad (11)$$

where $|\otimes\rangle$ is the vacuum state with no photon in the two waveguides, and the state $|m, n\rangle$ ($m = 1, 2, 3$) denotes that the atom is in the state $|m\rangle$ and the extra cavity contains n photons. In addition, $f(x)$, β , and ζ correspond to amplitudes. From the time-independent Schrödinger equation $H_e |\Psi_e\rangle = E_k |\Psi_e\rangle$, by equating the coefficients of $c_e^\dagger(x) |\otimes\rangle |1, n\rangle$, $|\otimes\rangle |2, n\rangle$, and $|\otimes\rangle |3, n-1\rangle$, respectively, we obtain the equations for the amplitudes

$$\left(-i\frac{\partial}{\partial x} - \delta_k^n\right) f_k(x) + \sqrt{\gamma}\beta\delta(x) = 0, \quad (12a)$$

$$-\Delta_k^n\beta + \sqrt{\gamma}f_k(0) + \sqrt{n}\lambda\zeta = 0, \quad (12b)$$

$$-(\Delta_k^n + \Delta_a)\zeta + \sqrt{n}\lambda\beta = 0. \quad (12c)$$

Where $\delta_k^n = E_k - n\omega_a$ represents the eigenfrequency of the incident single photon, i.e., νk , and the detuning $\Delta_k^n = \delta_k^n - \omega_2$, $\Delta_a = \omega_a - \omega_{32}$ describes the energy difference between the eigenfrequency of the incident single photon νk and $|2\rangle \leftrightarrow |1\rangle$, the extra cavity frequency ω_a and $|3\rangle \leftrightarrow |2\rangle$, respectively. Eq. (12c) can be rewritten as

$$\zeta = \frac{\sqrt{n}\lambda}{\Delta_k^n + \Delta_a}\beta, \quad (13)$$

substituting Eq. (13) into Eq. (12b) yields

$$\beta = \sqrt{\gamma}\delta(x) \frac{(\Delta_k^n + \Delta_a)}{\Delta_k^n(\Delta_k^n + \Delta_a) - n\lambda^2} f_k(x), \quad (14)$$

again, applying the constraint Eq. (14) to Eq. (12a) yields

$$\left[\left(-i\frac{\partial}{\partial x} - \delta_k^n\right) + V\delta(x)\right] f_k(x) = 0, \quad (15)$$

where we have introduced the energy-dependent δ -like potentials $V \equiv \gamma \frac{(\Delta_k^n + \Delta_a)}{\Delta_k^n(\Delta_k^n + \Delta_a) - n\lambda^2}$. It is clear that when $n = 0$, the potential is the result in Ref.⁴⁶, at the incident energy resonance, i.e., $\Delta_k^n = 0$, V goes to infinity. Notice that if the a-mode contains photons, that is, $n \neq 0$, but the a-mode photon resonantly drives the atomic transition, i.e., $\Delta_a = 0$, the potential equals zero. More broadly speaking, if $\Delta_k^n + \Delta_a = 0$, then $V \rightarrow 0$; if

$\Delta_k^n(\Delta_k^n + \Delta_a) - n\lambda^2 = 0$, then $V \rightarrow \infty$. Therefore, we can regulate the effective potential V from 0 to ∞ by the parameters of the a-mode field. Obviously, the plane-wave solution $f_k(x)$ is sufficient to satisfy Eq. (17)

$$f_k(x) = P_k(x) [\Theta(-x) + t_{k,e}\Theta(x)], \quad (16)$$

$$t_{k,e} = \frac{\Delta_k^n - \frac{n\lambda^2}{\Delta_k^n + \Delta_a} - i\frac{\gamma}{2}}{\Delta_k^n - \frac{n\lambda^2}{\Delta_k^n + \Delta_a} + i\frac{\gamma}{2}}. \quad (17)$$

In all the following calculations, we set $f_k(0) = \frac{1}{2}[f_k(0^+) + f_k(0^-)]$ ^{69,70}, and $\Theta(x)$ is the step function. And we assume that in the incident interval, the incoming wave functions consist entirely of plane waves^{32,69,70}, that is, for $x < 0$, $f_k(x) = P_k(x) = \frac{1}{\sqrt{2\pi}}e^{ikx}$.

Note that $t_{k,e}$ is the transmission coefficient for the interacting model because the even mode is extremely chiral, $|t_{k,e}|^2 = 1$. In the actual operation, for a normalized state

$$|\Psi_{in}\rangle_k = |\Psi_{in}\rangle_{G_p} = \int dx \frac{1}{\sqrt{2\pi}} e^{ikx} G_p^\dagger(x) |\otimes\rangle |1, n\rangle, \quad (18)$$

which considers a monochromatic right-going ($G = R$) or left-going ($G = L$) photon incident from the waveguide p , the out-state is

$$|\Psi_{out}\rangle_k = t_{pg,k}^p |\Psi_{out}\rangle_{G_p} + r_{pg,k}^p |\Psi_{out}\rangle_{\bar{G}_p} + t_{pg,k}^{\bar{p}} |\Psi_{out}\rangle_{G_{\bar{p}}} + r_{pg,k}^{\bar{p}} |\Psi_{out}\rangle_{\bar{G}_{\bar{p}}}. \quad (19)$$

where the four-mode transmission amplitudes $t_{pg,k}^p, t_{pg,k}^{\bar{p}}$ and reflection amplitudes $r_{pg,k}^p, r_{pg,k}^{\bar{p}}$ are

$$t_{pg,k}^p = \frac{\gamma p_g U_k}{\gamma} + 1, \quad (20a)$$

$$r_{pg,k}^p = \frac{\sqrt{\gamma p_g \gamma p_{\bar{g}}}}{\gamma} U_k, \quad (20b)$$

$$t_{pg,k}^{\bar{p}} = \frac{\sqrt{\gamma p_g \gamma p_{\bar{g}}}}{\gamma} U_k, \quad (20c)$$

$$r_{pg,k}^{\bar{p}} = \frac{\sqrt{\gamma p_g \gamma p_{\bar{g}}}}{\gamma} U_k. \quad (20d)$$

To simplify, we introduce the scattering factors U_k , expressed as

$$U_k \equiv t_{k,e} - 1 = \frac{-i\gamma(\Delta_k^n + \Delta_a)}{(\Delta_k^n(\Delta_k^n + \Delta_a) - n\lambda^2) + i\frac{\gamma}{2}(\Delta_k^n + \Delta_a)}. \quad (21)$$

The corresponding four scattering coefficients are defined as $T_p \equiv |t_{pg,k}^p|^2$, $R_p \equiv |r_{pg,k}^p|^2$, $T_{\bar{p}} \equiv |t_{pg,k}^{\bar{p}}|^2$, $R_{\bar{p}} \equiv |r_{pg,k}^{\bar{p}}|^2$. T_p and R_p are the transmission and reflection coefficients of waveguide p ; $T_{\bar{p}}$ and $R_{\bar{p}}$ are the transmission and reflection coefficients of waveguide \bar{p} ; $\bar{p} \neq p$. If the photon is transferred from waveguide p to waveguide \bar{p} , the transfer coefficient is denoted by T , which is $T \equiv T_{\bar{p}} + R_{\bar{p}}$. The single-photon scattering probabilities T_p, R_p , and T with respect to detuning Δ_a

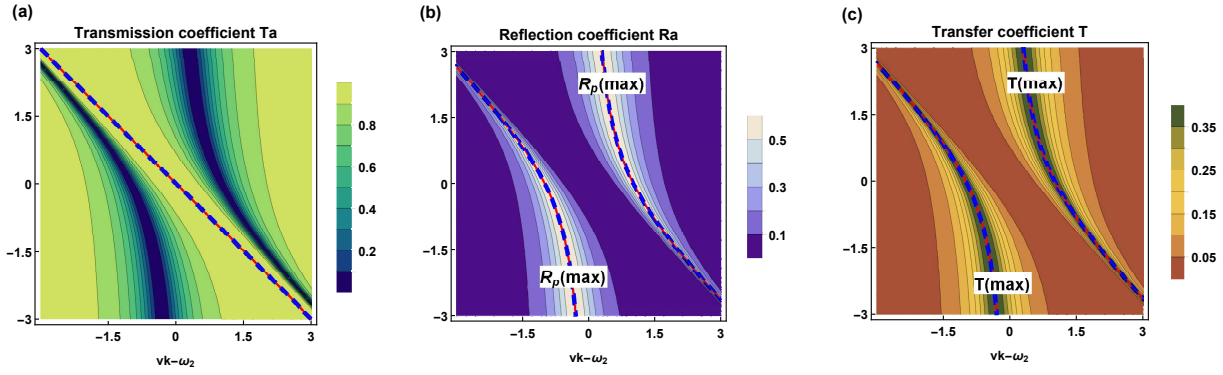


FIG. 2. (Color online) Single photon routing probability: (a) Transmission, (b) Reflection, and (c) Transfer coefficients versus the detuning Δ_k^n and Δ_a . We set $\gamma_{pg}/\gamma = 1/2$, $\gamma_{p\bar{g}}/\gamma = 0.3$, $\gamma_{\bar{p}g}/\gamma = \gamma_{\bar{p}\bar{g}}/\gamma = 0.1$, $\lambda/\gamma = 1$, and $n = 1$. All the parameters but n are in units of γ .

and Δ_k^n are shown in Fig. 2. The red-blue asymptotic line in Fig. 2(a) implies that the incident photon completely transmits ($T_p = 1$) for $\Delta_k^n + \Delta_a = 0$. This is because the incident photon induces the photon transition in the extra cavity, causing the atom to directly transition to the highest state $|3\rangle$, i.e., $\omega_3 = \omega_a + vk$, resulting in photon-induced tunneling (PIT), as shown in Fig. 3(a). Besides, the red-blue asymptotic line in

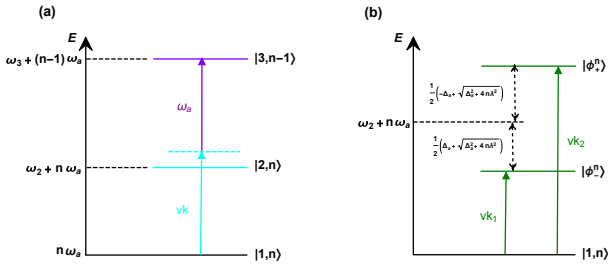


FIG. 3. (Color online) The energy-level diagram shows a single incident photon-induced tunneling (PIT) in (a), and in the dressed state representation, it can be considered an effective V-type atom with the energy-level diagram shown in (b).

Fig. 2(b)-(c) represents the incident photon that can't transmit ($T_p = 0$), and the reflect coefficient (R_p) and transfer coefficient (T) reach their maximum for $\Delta_k^n (\Delta_k^n + \Delta_a) - n\lambda^2 = 0$. It can be seen that the routing probability attains its maximum $R_p = 60\%$ and $T = 40\%$ at two red-blue asymptotic lines. Generally, the maximum routing probability (i.e., the routing peak) corresponds with the resonant input photons (i.e., $\Delta_k^n = 0$)⁴⁶. The splitting and shifting of the routing peaks in Fig. 2(b)-(c) show the effects of the Rabi splitting, which is caused by the coupling between the extra cavity and the atom. It may be better understood by substitution of the dressed state, that is, under n excitation subspaces, the coupling model of the extra cavity mode a and atom $|3\rangle \leftrightarrow |2\rangle$ is equivalent to $H_p^n = E_+^n |\phi_+^n\rangle \langle \phi_+^n| + E_-^n |\phi_-^n\rangle \langle \phi_-^n|$. Thus, our emitter can be considered a V-type system in the dressed state representation, as shown in Fig. 3(b). The effective transition $|1, n\rangle \leftrightarrow |\phi_{\pm}^n\rangle$ can be derived.

Fig. 3(a) shows the structure of the quantum emitter. The state $|3, n-1\rangle$ does not appear when the initial state of the ex-

tra cavity is in a vacuum state and the atom is in the ground state. At this time, it's impossible for the atom to transition from the state $|2\rangle$ to the state $|3\rangle$, and then the frequency corresponding to this particular tunnel route does not appear. To put it another way, under the dressed state appearance, as shown in Fig. 3(b), only the dressed state $|\phi_+^n\rangle$ plays a role at this point, and the emitter is equivalent to a two-level atom. Note that the tunneling routing points in Fig. 3(a) must exist once the extra cavity contains photons, while Fig. 3(b) needs to be discussed in detail. The Rabi splitting $\Omega_n(\Delta_a) = \sqrt{\Delta_a^2 + 4n\lambda^2}$ indicates that the single-photon transport properties are influenced by those parameters of the Jaynes-Cummings-like model, such as the detuning Δ_a , atom-cavity coupling strengths λ , and the number of photons n in the extra cavity.

In Fig. 4, we consider that λ and γ have the same order of magnitude, such as $\lambda = \gamma$. In Fig. 4(a), we plot the transmission spectra of a single photon at $\Delta_a = 0, 1.5$, and 4 , respectively. The figure shows that each value Δ_a has two different valleys and that the value determines the spectrum's symmetric or asymmetric properties. When $\Delta_a = 0$, T_p can show symmetry as a function of $vk - \omega_2$. With the increase of Δ_a , the symmetry of the spectrum is broken. The left valley shifts to the left, and the line width becomes narrower and sharper. Also, the right valley shifts to the left, infinitely close to zero, but does not cross zero on the left axis. Although the line width of the right valley increases with increasing Δ_a , it does not exceed the limit $\gamma/2$, which is the decay width of the atom. In addition, Fig. 4(b) shows that the larger the Δ_a , the lower the transmittance at the resonance. When Δ_a is large enough, that the number of photons in the extra cavity has almost no effect on the single-photon transmittance because the extra cavity is almost decoupled from the atom at this point, as shown in Fig. 4(c). All of this can be explained by the dressed states in Fig. 3(b), it is well known that in the large-detuning case, i.e., $\Delta_a \gg \sqrt{n}\lambda$. The dressed states $|\phi_{\pm}^n\rangle$ can be approximately written as: $|\phi_+^n\rangle \approx |2, n\rangle - \frac{\sqrt{n}\lambda}{\Delta_a} |3, n-1\rangle$; $|\phi_-^n\rangle \approx |3, n-1\rangle + \frac{\sqrt{n}\lambda}{\Delta_a} |2, n\rangle$ ⁷¹. The corresponding effective coupling strengths are $\gamma_+^n \approx \frac{\Delta_a^2}{\Delta_a^2 + n\lambda^2} \gamma$, $\gamma_-^n \approx \frac{\sqrt{n}\lambda}{\Delta_a} \gamma_+^n \approx \sqrt{n}\lambda \frac{\Delta_a}{\Delta_a^2 + n\lambda^2} \gamma$, respectively. Therefore, as the Δ_a increases, the line width of the left valley becomes sharper and sharper, and the line width

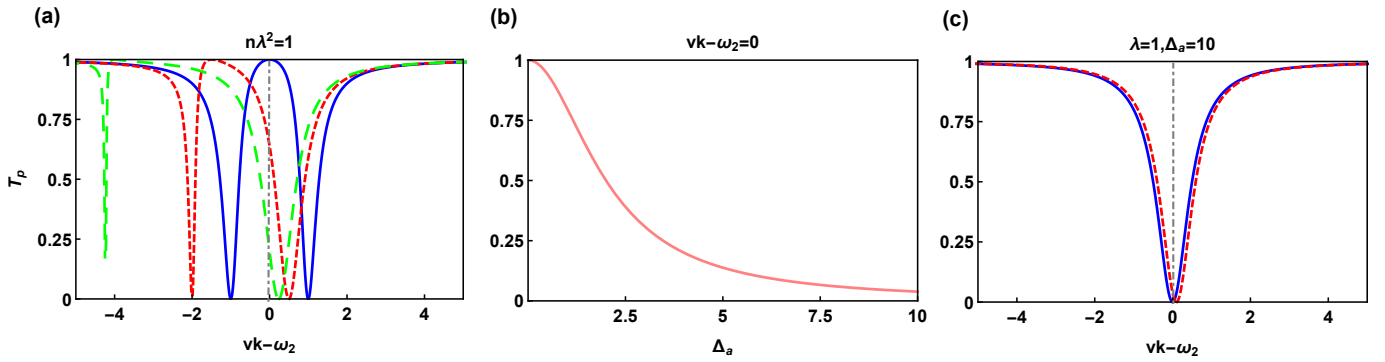


FIG. 4. (Color online) Transmission of a single photon against the detuning $vk - \omega_2$ in (a), (c), and against the detuning Δ_a in (b). The blue solid, red dashed, and green long dashed lines in panels (a) denote that the detuning Δ_a is taken as 0, 1.5, and 4, respectively. The black dotted dashed line in the middle of (a) represents the intersection of the three conditions when the incident resonant frequency. (b) is the slice diagram at this time. We consider $n = 1$ in (a), (b), and (c), where $n = 0$ (blue solid line) and $n = 1$ (red dashed line). Other parameters are set as follows: $\gamma_{pg}/\gamma = 1/2$, $\gamma_{p\bar{g}}/\gamma = 0.3$, $\gamma_{\bar{p}g}/\gamma = \gamma_{\bar{p}\bar{g}}/\gamma = 0.1$, $\lambda/\gamma = 1$. All the parameters but n are in units of γ .

of the right valley becomes closer and closer to $\gamma/2$. In the $\frac{\Delta_a}{\sqrt{n}\lambda} \rightarrow \infty$ limit, it is difficult for the system to transition from the state $|2, n\rangle$ to the state $|3, n-1\rangle$. At this point, there is no significant difference in whether the extra cavity contains photons or not, and the system is equivalent to a two-level emitter. Of course, all of these values always stayed within the rules of $|\Delta_a| \ll \omega_a + \omega_{32}$, and $\sqrt{n}\lambda \ll \min\{\omega_a, \omega_{32}\}$. Then one obtains the similar Jaynes-Cummings Hamiltonian $\omega_a a^\dagger a + \omega_2 \sigma_{22} + \omega_3 \sigma_{33} + \lambda a^\dagger \sigma_{23} + H.c.$

Fig. 4 shows the property of the single-photon transmission spectrum for $\Delta_a > \sqrt{n}\lambda$, while Fig. 5 shows the change that occurs in the transmission spectrum for $\Delta_a < \sqrt{n}\lambda$. As shown in Fig. 5(a), by increasing the number of photons n in the extra cavity (expanding Rabi splitting), the window of the transmission spectrum T_p is widened, and the spectral line shape tends to be symmetrical. In Fig. 5(b), we compare the different transmissions that vary with n when $\Delta_a = 1, 5$, and 10. The figure shows that large transmission can be achieved with a tiny Δ_a and a larger number of photons, n . This means that under these values, the effective coupling strength $\sqrt{n}\lambda$ of the transition $|2, n\rangle \leftrightarrow |3, n-1\rangle$ is large enough, and the detuning Δ_a between the bare states $|2, n\rangle$ and $|3, n-1\rangle$ is small enough, so the transition probability between $|2, n\rangle \leftrightarrow |3, n-1\rangle$ is much greater than the transition probability between $|2, n\rangle \leftrightarrow |1, n\rangle$. As for the case where the splitting width is less than the decay rate of the emitter, i.e., $\Omega_n(\Delta_a) < \gamma/2$, we will not elaborate here because the two decorated states are very close to each other, putting higher requirements on experimental observation.

In this paper, we have studied the single-photon routing in two 1D linear waveguide systems coupled with a three-level emitter with a cascade configuration. An extra cavity photon can drive the atomic transition from $|2\rangle$ to $|3\rangle$. So, if the emitter is in the ground state $|1\rangle$ initially, whether the cavity contains photons determines the effective configuration of the atom. Here, we have shown that complete transmission occurs if the extra cavity applied to the 3LS initially contains photons when $\Delta_k^n + \Delta_a = 0$. Besides, the routing peaks split-

ting and shifting in Fig. 4(a) show the influence of the Rabi splitting, which is caused by the coupling between the extra cavity and the atomic transition $|2\rangle \leftrightarrow |3\rangle$. In other words, we obtain an ATS line shape, and the transparency window can be controlled by the number of photons in the extra cavity. In addition, the location and width of the transmission valleys are tunable by adjusting the extra cavity. Consequently, the single-photon transport property depends on whether the extra cavity contains a photon or not. The single-photon transport can also be controlled by the number of photons in the extra cavity. Therefore, the proposal presented in this paper can be a competitive candidate for quantum routes. We hope that our proposal can provide a feasible approach to constructing various photonic networks and be used to do some further research, such as directional routing of a single photon with different frequencies and so on.

ACKNOWLEDGMENTS

This work was supported by NSFC Grants No.11975095, No.12075082, No.11935006, and the Science and Technology Innovation Program of Hunan Province (Grant No. 2020RC4047)

DATA AVAILABILITY

The data that support the findings of this study are available from the corresponding author upon reasonable request.

- ¹S. Bose, "Quantum Communication through an Unmodulated Spin Chain," *Phys. Rev. Lett.* **91**, 207901 (2003).
- ²P. Maunz, D. L. Moehring, S. Olmschenk, et al., "Quantum interference of photon pairs from two remote trapped atomic ions," *Nature Phys.* **3**, 538 (2007).
- ³Scully, M., Zubairy, M., *Quantum Optics* (Cambridge University Press, 1997).
- ⁴P. Y. Wen, K. T. Lin, A. F. Kockum, et al., "Large Collective Lamb Shift of Two Distant Superconducting Artificial Atoms," *Phys. Rev. Lett.* **123**, 233602 (2019).

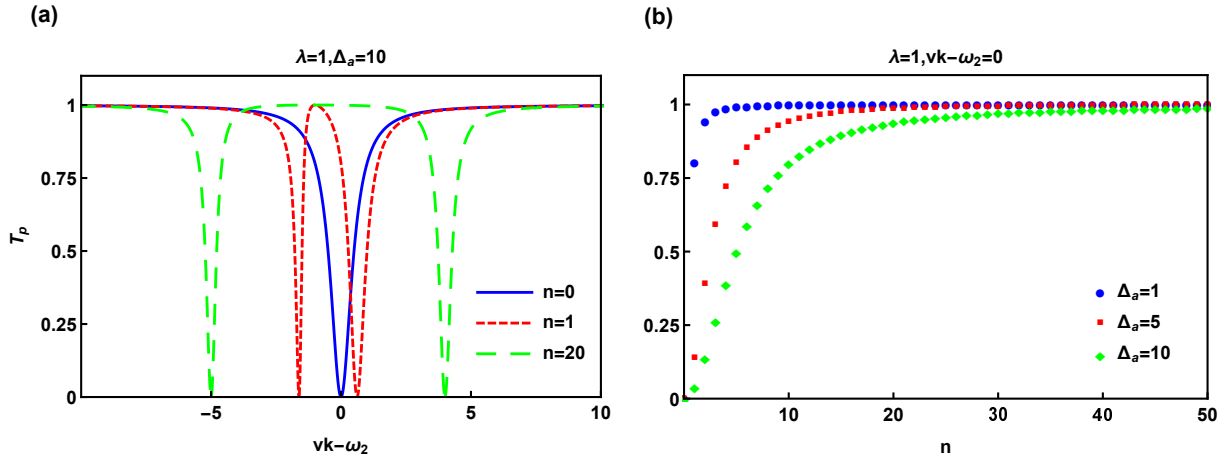


FIG. 5. (Color online) Transmission probability T_p as a function of $vk - \omega_2$ for three different initial extra cavity photon states in (a). State-1: vacuum state (blue solid line); State-2: single photon state (red dashed line); State-3: 20-photon state (green long dashed line). We consider $\Delta_a = \lambda = \gamma$ in panel (a). T_p as a function of n for $\Delta_a = 1$ (blue point symbol), $\Delta_a = 5$ (red square symbol), $\Delta_a = 10$ (green rhombus symbol) in panel (b), and the energy of the incident photon resonates with the emitter, i.e., $vk - \omega_2 = 0$. The other parameters remain the same as in Fig. 4.

- ⁵L. Zhou, Z. R. Gong, Y. X. Liu, et al., “Controllable Scattering of a Single Photon inside a One-Dimensional Resonator Waveguide,” *Phys. Rev. Lett.* **101**, 100501 (2008).
- ⁶L. Zhou, S. Yang, Y. X. Liu, et al., “Quantum Zeno switch for single-photon coherent transport,” *Phys. Rev. A* **80**, 062109 (2009).
- ⁷L. Zhou, L. P. Yang, Y. Li, et al., “Quantum Routing of Single Photons with a Cyclic Three-Level System,” *Phys. Rev. Lett.* **111**, 103604 (2013).
- ⁸W. B. Yan, H. Fan, “Single-photon quantum router with multiple output ports,” *Sci. Rep.* **4**, 4820 (2014).
- ⁹D. C. Yang, M. T. Cheng, X. S. Ma, et al., “Phase-modulated single-photon router,” *Phys. Rev. A* **98**, 063809 (2018).
- ¹⁰Y. T. Zhu, W. Z. Jia, “Single-photon quantum router in the microwave regime utilizing double superconducting resonators with tunable coupling,” *Phys. Rev. A* **99**, 063815 (2019).
- ¹¹L. Zhou, H. Dong, Y. X. Liu, et al., “Quantum super-cavity with atomic mirrors,” *Phys. Rev. A* **78**, 063827 (2008).
- ¹²Z. L. Wang, Y. K. Wu, Z. H. Bao, et al., “Experimental Realization of a Deterministic Quantum Router with Superconducting Quantum Circuits,” *Phys. Rev. Appl.* **15**, 014049 (2021).
- ¹³I. C. Hoi, C. M. Wilson, G. Johansson, et al., “Demonstration of a Single-Photon Router in the Microwave Regime,” *Phys. Rev. Lett.* **107**, 073601 (2011).
- ¹⁴X. Gu, A. F. Kockum, A. Miranowicz, et al., “Microwave photonics with superconducting quantum circuits,” *Phys. Rep.* **1**, 718719 (2017).
- ¹⁵H. C. Sun, Y. X. Liu, H. Ian, et al., “Electromagnetically induced transparency and Autler-Townes splitting in superconducting flux quantum circuits,” *Phys. Rev. A* **89**, 063822 (2014).
- ¹⁶Y. X. Liu, X. W. Xu, A. Miranowicz, et al., “From blockade to transparency: Controllable photon transmission through a circuit-QED system,” *Phys. Rev. A* **89**, 043818 (2014).
- ¹⁷X. Wang, A. Miranowicz, H. R. Li, et al., “Two-color electromagnetically induced transparency via modulated coupling between a mechanical resonator and a qubit,” *Phys. Rev. A* **98**, 023821 (2018).
- ¹⁸G. S. Agarwal, S. M. Huang, “Optomechanical systems as single-photon routers,” *Phys. Rev. A* **85**, 021801 (2012).
- ¹⁹X. Li, W. Z. Zhang, B. Xiong, et al., “Single-photon multi-ports router based on the coupled cavity optomechanical system,” *Sci. Rep.* **6**, 39343 (2016).
- ²⁰Y. Chang, T. Shi, Y. X. Liu, et al., “Multistability of electromagnetically induced transparency in atom-assisted optomechanical cavities,” *Phys. Rev. A* **83**, 063826 (2011).
- ²¹H. Wang, X. Gu, Y. X. Liu, et al., “Optomechanical analog of two-color electromagnetically-induced transparency: Photon transmission through an optomechanical device with a two-level system,” *Phys. Rev. A* **90**, 023817 (2014).
- ²²H. Jing, S. K. Ödemir, Z. Geng, et al., “Optomechanically-induced transparency in parity-time-symmetric microresonators,” *Sci. Rep.* **5**, 9663 (2015).
- ²³D. G. Lai, X. Wang, W. Qin, et al., “Tunable optomechanically induced transparency by controlling the dark-mode effect,” *Phys. Rev. A* **102**, 023707 (2020).
- ²⁴I. Shomroni, S. Rosenblum, Y. Lovsky, et al., “All-optical routing of single photons by a one-atom switch controlled by a single photon,” *Science* **345**, 903 (2014).
- ²⁵J. T. Shen, S. H. Fan, “Coherent Single Photon Transport in a One-Dimensional Waveguide Coupled with Superconducting Quantum Bits,” *Phys. Rev. Lett.* **95**, 213001 (2005).
- ²⁶X. M. Li, L. F. Wei, “Designable single-photon quantum routings with atomic mirrors,” *Phys. Rev. A* **92**, 063836 (2015).
- ²⁷K. Y. Xia, F. Jelezko, J. Twamley, “Quantum routing of single optical photons with a superconducting flux qubit,” *Phys. Rev. A* **97**, 052315 (2018).
- ²⁸M. Ahumada, P. A. Orellana, F. D. Adame, et al., “Tunable single-photon quantum router,” *Phys. Rev. A* **99**, 033827 (2019).
- ²⁹B. Poudyal, I. M. Mirza, “Collective photon routing improvement in a dissipative quantum emitter chain strongly coupled to a chiral waveguide QED ladder,” *Phys. Rev. Research* **2**, 043048 (2020).
- ³⁰J. T. Shen, S. H. Fan, “Strongly correlated multiparticle transport in one dimension through a quantum impurity,” *Phys. Rev. A* **76**, 062709 (2007).
- ³¹J. T. Shen, S. H. Fan, “Strongly Correlated Two-Photon Transport in a One-Dimensional Waveguide Coupled to a Two-Level System,” *Phys. Rev. Lett.* **98**, 153003 (2007).
- ³²H. X. Zheng, D. J. Gauthier, H. U. Baranger, “Waveguide QED: Many-body bound-state effects in coherent and Fock-state scattering from a two-level system,” *Phys. Rev. A* **82**, 063816 (2010).
- ³³M. Bradford, J. T. Shen, “Numerical approach to statistical properties of resonance fluorescence,” *Opt. Lett.* **39**, 5558 (2014).
- ³⁴S. H. Fan, Ş. E. Kocabaş, J. T. Shen, “Input-output formalism for few-photon transport in one-dimensional nanophotonic waveguides coupled to a qubit,” *Phys. Rev. A* **82**, 063821 (2010).
- ³⁵Y. C. Shen, J. T. Shen, “Photonic-Fock-state scattering in a waveguide-QED system and their correlation functions,” *Phys. Rev. A* **92**, 033803 (2015).
- ³⁶W. J. Lin, Y. Lu, P. Y. Wen, et al., “Deterministic Loading of Microwaves onto an Artificial Atom Using a Time-Reversed Waveform,” *Nano Lett.* **22**, 8137–8142 (2022).
- ³⁷J. Q. Liao, Z. R. Gong, L. Zhou, et al., “Controlling the transport of single photons by tuning the frequency of either one or two cavities in an array of

- coupled cavities,” *Phys. Rev. A* **81**, 042304 (2010).
- ³⁸J. Lu, L. Zhou, L. M. Kuang, et al., “Single-photon router: Coherent control of multichannel scattering for single photons with quantum interferences,” *Phys. Rev. A* **89**, 013805 (2014).
- ³⁹W. B. Yan, H. Fan, “Control of single-photon transport in a one-dimensional waveguide by a single photon,” *Phys. Rev. A* **90**, 053807 (2014).
- ⁴⁰W. Qin, F. Nori, “Controllable single-photon transport between remote coupled-cavity arrays,” *Phys. Rev. A* **93**, 032337 (2016).
- ⁴¹Y. L. Wang, Y. Yang, J. Lu, et al., “Photon transport and interference of bound states in a one-dimensional waveguide,” *Opt. Express* **30**(9), 14048–14060 (2022).
- ⁴²C. G. Ballester, E. Moreno, F. J. Garcia-Vidal, et al., “Nonreciprocal few-photon routing schemes based on chiral waveguide-emitter couplings,” *Phys. Rev. A* **94**, 063817 (2016).
- ⁴³H. Ian, Y. X. Liu, F. Nori, “Tunable electromagnetically induced transparency and absorption with dressed superconducting qubits,” *Phys. Rev. A* **81**, 063823 (2010).
- ⁴⁴B. Peng, S. K. Özdemir, W. J. Chen, et al., “What is and what is not electromagnetically induced transparency in whispering-gallery microcavities,” *Nature Communications* **5**, 6082 (2014).
- ⁴⁵Q. C. Liu, T. F. Li, X. Q. Luo, et al., “Method for identifying electromagnetically induced transparency in a tunable circuit quantum electrodynamics system,” *Phys. Rev. A* **93**, 053838 (2016).
- ⁴⁶Y. Yang, J. Lu, L. Zhou, “Few-photon routing via chiral light-matter couplings,” *Communications in Theoretical Physics* **74**(2), 025101 (2022).
- ⁴⁷P. Y. Wen, A. F. Kockum, H. Ian, et al., “Reflective Amplification without Population Inversion from a Strongly Driven Superconducting Qubit,” *Phys. Rev. Lett.* **120**, 063603 (2018).
- ⁴⁸P. Y. Wen, O. V. Ivakhnenko, M. A. Nakonechnyi, et al., “Landau-Zener-Stueckelberg-Majorana interferometry of a superconducting qubit in front of a mirror,” *Phys. Rev. B* **102**, 075448 (2020).
- ⁴⁹M. P. Liul, C. H. Chien, C. Y. Chen, et al., “Coherent dynamics of a photon-dressed qubit,” *Phys. Rev. B* **107**, 195441 (2023).
- ⁵⁰S. S. Apostolov, Z. A. Maizelis, M. A. Sorokina, et al., “Self-induced tunable transparency in layered superconductors,” *Phys. Rev. B* **82**, 144521 (2010).
- ⁵¹X. W. Xu, Y. J. Zhao, H. Wang, et al., “Quantum nonreciprocity in quadratic optomechanics,” *Photonics Res.* **8**(2), 143 (2020).
- ⁵²X. W. Xu, Y. Li, B. Li, et al., “Nonreciprocity via Nonlinearity and Synthetic Magnetism,” *Phys. Rev. Appl.* **13**(4), 044070 (2020).
- ⁵³Y. F. Jiao, S. D. Zhang, Y. L. Zhang, et al., “Nonreciprocal Optomechanical Entanglement against Backscattering Losses,” *Phys. Rev. Lett.* **125**(14), 143605 (2020).
- ⁵⁴F. X. Sun, D. Mao, Y. T. Dai, et al., “Phase control of entanglement and quantum steering in a three-mode optomechanical system,” *New J. Phys.* **19**(12), 123039 (2017).
- ⁵⁵Z. Wang, Y. D. Chong, J. D. Joannopoulos, et al., “Observation of unidirectional backscattering-immune topological electromagnetic states,” *Nature (London)* **461**(7265), 772–775 (2009).
- ⁵⁶Y. Poo, R. X. Wu, Z. Lin, et al., “Experimental Realization of Self-Guiding Unidirectional Electromagnetic Edge States,” *Phys. Rev. Lett.* **106**(9), 093903 (2011).
- ⁵⁷S. A. Skirlo, L. Lu, Y. Igarashi, et al., “Experimental Observation of Large Chern Numbers in Photonic Crystals,” *Phys. Rev. Lett.* **115**(25), 253901 (2015).
- ⁵⁸R. Jones, G. Buonaiuto, B. Lang, et al., “Collectively Enhanced Chiral Photon Emission from an Atomic Array near a Nanofiber,” *Phys. Rev. Lett.* **124**(9), 093601 (2020).
- ⁵⁹P. Roushan, C. Neill, A. Megrant, et al., “Chiral ground-state currents of interacting photons in a synthetic magnetic field,” *Nat. Phys.* **13**(2), 146–151 (2017).
- ⁶⁰E. Sanchez-Burillo, C. Wan, D. Zueco, et al., “Chiral quantum optics in photonic sawtooth lattices,” *Phys. Rev. Res.* **2**(2), 023003 (2020).
- ⁶¹T. Ramos, H. Pichler, A. J. Daley, et al., “Quantum Spin Dimers from Chiral Dissipation in Cold-Atom Chains,” *Phys. Rev. Lett.* **113**(23), 237203 (2014).
- ⁶²C. Sayrin, C. Junge, R. Mitsch, et al., “Nanophotonic Optical Isolator Controlled by the Internal State of Cold Atoms,” *Phys. Rev. X* **5**(4), 041036 (2015).
- ⁶³S. R. Sathyamoorthy, L. Tornberg, A. F. Kockum, et al., “Quantum non-demolition detection of a propagating microwave photon,” *Phys. Rev. Lett.* **112**, 093601 (2014).
- ⁶⁴K. Y. Bliokh, F. J. Rodríguez-Fortuño, F. Nori, et al., “Spin-orbit interactions of light,” *Nat. Photonics* **9**, 796 (2015).
- ⁶⁵K. Y. Bliokh, F. Nori, “Transverse and longitudinal angular momenta of light,” *Phys. Rep.* **592**, 1 (2015).
- ⁶⁶T. Ramos, H. Pichler, A. J. Daley, et al., “Quantum spin dimers from chiral dissipation in cold-atom chains,” *Phys. Rev. Lett.* **113**, 237203 (2014).
- ⁶⁷P. Lodahl, S. Mahmoodian, S. Stobbe, et al., “Chiral quantum optics,” *Nature* **541**, 473 (2017).
- ⁶⁸P. Longo, P. Schmitteckert, K. Busch, “Few-Photon Transport in Low-Dimensional Systems: Interaction-Induced Radiation Trapping,” *Phys. Rev. Lett.* **104**(2), 023602 (2010).
- ⁶⁹A. Nishino, T. Imamura, N. Hatano, “Exact Scattering Eigenstates, Many-Body Bound States, and Nonequilibrium Current in an Open Quantum Dot System,” *Phys. Rev. Lett.* **102**, 146803 (2009).
- ⁷⁰T. Imamura, A. Nishino, N. Hatano, “Entanglement generation through an open quantum dot: Exact two-electron scattering state in the Anderson model,” *Phys. Rev. B* **80**, 245323 (2009).
- ⁷¹X. Gu, S. N. Huai, F. Nori, et al., “Polariton states in circuit QED for electromagnetically induced transparency,” *Phys. Rev. A* **93**(6), 063827 (2016).